

ECLIPSING STELLAR BINARIES IN THE GALACTIC CENTER

GONGJIE LI ¹, IDAN GINSBURG ¹, SMADAR NAOZ ², ABRAHAM LOEB ¹¹ Harvard-Smithsonian Center for Astrophysics, The Institute for Theory and Computation,
60 Garden Street, Cambridge, MA 02138, USA² Physics and Astronomy, UCLA, Los Angeles, CA 90095, USA*Draft version January 27, 2023*

ABSTRACT

Compact stellar binaries are expected to survive in the dense environment of the Galactic Center. The stable binaries may undergo Kozai-Lidov oscillations due to perturbations from the central supermassive black hole (Sgr A*), yet the General Relativistic precession can suppress the Kozai-Lidov oscillations and keep the stellar binaries from merging. However, it is challenging to resolve the binary sources and distinguish them from single stars. The close separation of the stable binaries allow higher eclipse probabilities. Here, we consider the massive star SO2 as an example and calculate the probability of detecting eclipses, assuming it is a binary. We find that the eclipse probability is $\sim 30 - 50\%$, reaching higher values when the stellar binary is more eccentric or highly inclined relative to its orbit around Sgr A*.

1. INTRODUCTION

Observations of the inner region of our Milky Way provide valuable information on the stellar population and the supermassive black hole (SMBH), Sgr A*, in the Galactic Center, and allow a unique opportunity to study the interactions of the SMBH and its surrounding stars. There are three detected stellar binaries within ~ 0.2 pc of the Galactic Center: IRS16W (Ott et al. 1999; Martins et al. 2006), IRS 16NE and E60 (Pfahl et al. 2014). IRS16W and E60 are eclipsing binaries and IRS 16NE is a long period spectroscopic binary. Based on these three detections, it has been estimated that the binary fraction in the Galactic Center is similar to that of a young stellar cluster (Pfahl et al. 2014). The binary population plays important roles in the dynamical processes at the Galactic Center. For instance, the binaries contribute to the relaxation of the Galactic Center (Alexander & Hopman 2009), and they explain the origin of the young stellar population in the galactic center, such as the S-stars (Antonini & Merritt 2013), the hypervelocity stars (e.g., Hills 1988; Yu & Tremaine 2003; Ginsburg & Loeb 2007; Perets 2009) and the G1 and G2 clouds (Witzel et al. 2014; Stephan et al. 2016; Witzel et al. 2017). Moreover, the existence of a binary population may yield an underestimation of the GC stellar disk membership (Naoz & Ghez in prep.).

Long term stability requires that binaries in the GC have a tight configuration in reference to their orbit around the SMBH. In particular, Kozai-Lidov oscillations (Kozai 1962; Lidov 1962) due to perturbations from Sgr A* may excite the eccentricity of a stellar binary, reduce its pericenter distances, and lead to mergers of the binary components in the Galactic Center (Prodan et al. 2015; Naoz 2016; Stephan et al. 2016). Stephan et al. (2016) found that within 0.1 pc of the SMBH, $\sim 13\%$ of the initial binary population will merge in a few million years and $\sim 17\%$ will become unbound due to interactions with single stars. Moreover, 70% of the initial pop-

ulation will remain bound to a binary companion after a few million years.

It is not clear whether the observed stellar systems in the Galactic Center are single stars or binaries, due to the high resolution required to distinguish between these possibilities. The existence of S-stars poses challenges regarding their formation, as the strong tidal field from Sgr A* should inhibit the collapse and fragmentation of the parent molecular cloud (Morris 1993). Thus, migration of the stars after formation may be involved in the formation of such systems (Merritt et al. 2009; Perets & Gualandris 2010). The challenging detection of stellar binaries in the Galactic Center and in particular the identification of S-stars as stellar binaries will provide valuable information on both the formation of the S-stars and the dynamical processes in the Galactic Center.

Here, we consider the probability for the stable binaries to eclipse, which can help distinguish them from the single star systems. In particular, we use SO2 as an example, calculate the probability for its members to eclipse in §3, and present observational predictions in §4.

2. BINARIES IN THE GALACTIC CENTER

Binaries in the Galactic Center are difficult to resolve and distinguish from single stars. In this section, we address the probability for the binary components to eclipse each other, which is an approach to detect such binaries. As a proof-of-concept, we adopt SO2 as an example, since it has the best orbital constraints. The system configuration is shown in Figure 1. We use the subscript ‘SO2’ to denote the outer orbit of SO2 around Sgr A*. Following Gillessen et al. (2009), we set the semi-major axis $a_{SO2} = 1000$ AU, eccentricity $e_{SO2} = 0.9$, line of sight inclination $i_{SO2} = 134.87^\circ$, the mass of SO2 to be $15M_\odot$ and the mass of Sgr A* to be $4 \times 10^6 M_\odot$. $a < 1.08$ AU is needed for the stellar binary to avoid disruption in a circular orbit with eccentricity $e = 0$, whereas $a < 0.54$ AU when $e \rightarrow 1$.

Perturbations induced by Sgr A* generally excite the eccentricity of the stellar binary and can lead to mergers

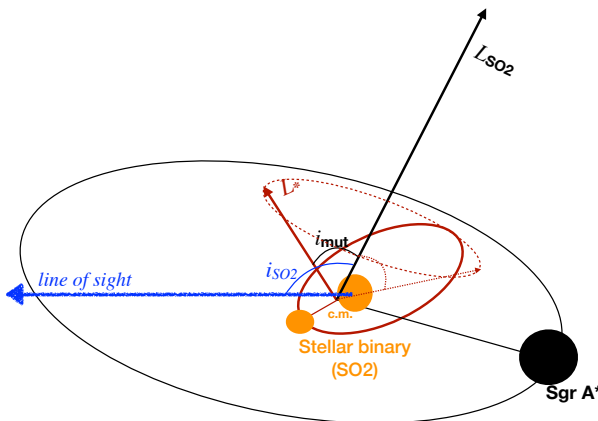


Figure 1. Hypothetical binary geometry for SO2. ‘c.m.’ denotes the center of mass of the binary. The inner orbit is the orbit of the binary components around the c.m., and the outer orbit is the orbit of SO2 around Sgr A*. i_{mut} denotes the mutual inclination between the two orbits. The dashed cone represents the orbital spin orientation with the same mutual inclination. The blue arrow delineates the line of sight. For SO2, the line of sight inclination is $i_{\text{SO2}} = 134.87^\circ$ (Gillessen et al. 2009).

of the stars (e.g., Stephan et al. 2016). For stellar binaries at the location of SO2, we find that binaries survive when the semi-major axis is $a = 0.1$ AU and $e \sim 0$, where the GR precession can suppress the Kozai-Lidov oscillations.

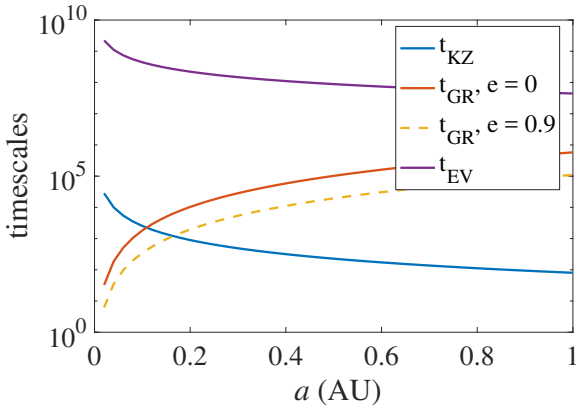


Figure 2. The precession timescales (t_{GR} and t_{KZ}) and the evaporation timescale (t_{EV}) for SO2. The GR precession timescale (t_{GR}) is shorter than the KZ oscillation timescale (t_{KZ}) when $a \lesssim 0.15$ AU. The evaporation timescale is much longer than the precession timescales for small a .

Figure 2 shows the relevant timescales of the SO2 system. The blue line represents the Kozai-Lidov timescale; the red and the yellow dashed lines represent the precession timescales of the stellar binary due to GR with orbital eccentricities of $e = 0$ and $e = 0.9$ separately (Naoz 2016). The stellar binaries could be dissociated (evaporated) through stellar encounters in the Galactic Center (Binney & Tremaine 1987). The evaporation timescale is shown by the purple line. The Kozai-Lidov oscillations can be suppressed when the GR precession timescale is shorter, and the stellar binary is stable against dissociation within the evaporation timescale. The relevant

equations can be found in Stephan et al. 2016.

Figure 2 shows that Kozai-Lidov oscillations can be suppressed when $a \lesssim 0.15$ AU, and stars with a larger semi-major axis can survive when the orbit is more eccentric. The evaporation timescale is much longer than the precession timescales and the lifetime of the stars for small stellar binary orbital semi-major axis. As an illustrative example, we consider the case with $a = 0.1$ AU.

3. ECLIPSE PROBABILITY

The eclipse probability of a stellar binary is $(R_1 + R_2)/a$, where R_1 and R_2 are the stellar radii (e.g., Pan & Loeb 2012). We obtain the eclipse probability of SO2 as a function of stellar mass ratio q , assuming a total mass for the stellar binary is $15M_\odot$, and following the mass-radius relation by Kippenhahn et al. (2012), where the radius $R \propto M^{0.57}$ for a stellar mass $M > 1M_\odot$, and $R \propto M^{0.8}$ for $M < 1M_\odot$. In addition to setting $a = 0.1$ AU as a default, we also calculate the probability when the stellar binary components are separated by the maximum of their Roche Lobe radii (i.e., one of the binary components is at its tidal limit). We follow Eggleton (1983) to obtain the tidal limit. The tidal disruption separation is $\sim 0.03 - 0.04$ AU depending on the binary mass ratio, with the largest value obtained when the binary mass ratio is ~ 0.57 .

Figure 3 shows the eclipse probability for the SO2 system. The blue line shows the case when the semi-major axis of the stellar binary is 0.1 AU, and the red line corresponds to the case where the stars are at their tidal disruption separation. The eclipse probability reaches a maximum of $\sim 75\%$ when one of the stars is at its tidal limit. The eclipse probability is then $\sim 20 - 30\%$ for $a \sim 0.1$ AU. Overall, the eclipse probability depends linearly on the semi-major axis of the stellar binary, and is weakly dependent on the binary mass ratio.

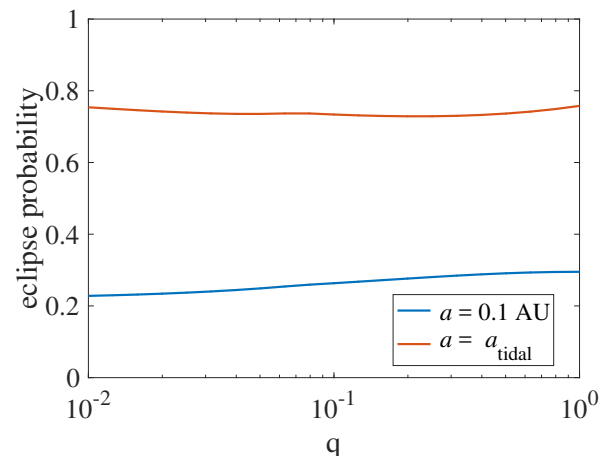


Figure 3. Eclipse probability of SO2. The eclipse probability reaches a maximum of $\sim 75\%$ when the binary components are at their tidal disruption separation. The probability is $\sim 25\%$ when $a = 0.1$ AU. The probability depends weakly on the mass ratio of the binary (q).

Both the eclipse probability and the orbital stability depend on the mutual inclination between the stellar bi-

nary and the orbit around Sgr A* (see Figure 1). In particular, the orientation of the stellar binary determines the probability for the stars to eclipse along the line of sight, as the eclipse probability is larger when the stellar binary is more likely to lie along the line of sight, namely for $i_{\text{mut}} \gtrsim i_{SO2} - 90^\circ$. Dynamically, the eccentricity excitation can be stronger when the stellar binary is more inclined from the orbit around Sgr A*. Next, we calculate the probability for the stellar binary to eclipse as a function of the mutual inclination between the stellar binary and their orbit around Sgr A*.

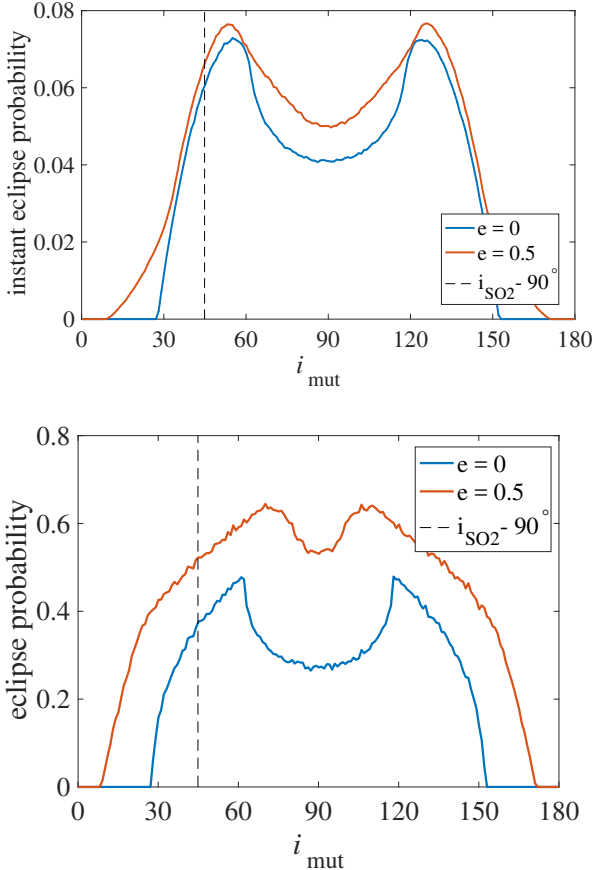


Figure 4. Upper panel: eclipse probability of SO2 as a function of mutual inclination between SO2 and orbit around Sgr A*. Lower panel: eclipse probability of SO2 over the orbital period as a function of the mutual inclination. We assume $a = 0.1$ AU.

Figure 4 illustrates the eclipse probability for SO2 as a function of the mutual inclination, where we assume the semi-major axis of the stellar binary is 0.1 AU. To calculate the eclipse probability, we set the longitude of node for SO2 to be $\Omega_{SO2} = 226.53^\circ$, the argument of pericenter to be $\omega_{SO2} = 64.98^\circ$ and the inclination to be $i_{SO2} = 134.87^\circ$ (Gillessen et al. 2009), and use Monte Carlo simulations with uniformly distributed mean anomaly, argument of pericenter and longitude of node for the stellar binary. i_{SO2} determines the probability distribution as a function of mutual inclination. The eclipse probability is larger when the stellar binary is more likely to lie along the line of sight, i.e., when $i_{\text{mut}} \gtrsim i_{SO2} - 90^\circ$, as shown in Figure 1. The dependence

on i_{mut} is symmetric around $i_{\text{mut}} = 90^\circ$. When i_{SO2} is near zero, the probability distribution is more centrally peaked around $i_{\text{mut}} = 90^\circ$, and when $i_{SO2} \sim 90^\circ$, the probability distribution peaks at $i_{\text{mut}} = 0^\circ$ and 180° . Ω_{SO2} and ω_{SO2} do not affect the eclipse probability.

The upper panel of Figure 4 shows the probability for the binary to eclipse at any instant of time (instantaneous eclipse probability) at a random stellar binary orbital phase, and the lower panel shows the probability over one orbital period (including all orbital phases). The blue lines correspond to a circular orbit, and the red lines correspond to an eccentric orbit. We set the mass ratio to be $q = 1$, but the results depends weakly on the mass ratio, as shown in Figure 3. Overall, the probability to eclipse is higher when the mutual inclination is larger. This is expected, since the orbital plane of SO2 is highly inclined in the sky plane. Specifically, the probabilities peak near $i_{\text{mut}} = i_{SO2} - 90^\circ$ and $i_{\text{mut}} = 270^\circ - i_{SO2}$, when the line of sight inclination is able to reach 90° . The peak i_{mut} is not exactly at $i_{SO2} - 90^\circ$ or $270^\circ - i_{SO2}$, because the size of the stellar binary allows a larger parameter region for eclipse when the line of sight inclination of the stellar binary is within $i_{\text{crit}} = (R_{*,1} + R_{*,2})/r_{12}$ from 90° , where r_{12} is the separation between the binary components. For an equal mass stellar binary separated by 0.1 AU, $i_{\text{crit}} = 17^\circ$. i_{crit} determines the minimum mutual inclination, $i_{\text{mut},\text{min}} = i_{SO2} - 90^\circ - i_{\text{crit}}$, when the eclipse probability is nonzero.

In addition, as shown in Figure 4, the instantaneous eclipse probability depends weakly on the stellar binary orbital eccentricity, since the distance averaging over the mean anomaly depends weakly on eccentricity, $(a(1+e^2/2))$. On the other hand, the eclipse probability over one orbital period is higher when the stellar orbit is more eccentric, since the eclipse probability is higher at the pericenter of the more eccentric orbit, when the distance between the binary members is shorter. Moreover, when the orbit is more eccentric, the mutual inclination associated with the peak in the probability is closer to polar ($i_{\text{mut}} \sim 90^\circ$). This is because the higher mutual inclination allows a larger phase space of orbital orientations, and the shorter distance between the stellar binary permits eclipses for a larger fraction of the possible orbital orientations. Averaging over the isotropic distribution of the stellar binary orbital orientation, we find that the total probability for the stellar binary to eclipse is 29.5% for a circular orbit, and is 52.4% for an eccentric orbit of $e = 0.5$.

Eccentricity excitation is weaker when the stellar binary masses are the same. Thus, we also consider the eclipse probability at larger distances with $q = 1$. The eclipse probability scales roughly linearly with the semi-major axis, dropping with larger a . For example, the eclipse probability is $\sim 5\%$ when $a = 0.5$ AU for large mutual inclination $60^\circ < i_{\text{mut}} < 120^\circ$. The eclipse probability peaks at around $\sim 48^\circ$ and $\sim 132^\circ$, with a value of $\sim 20\%$. The orbit is unstable when the mutual inclination is higher, corresponding to the configuration that is more likely to eclipse. Thus, the total eclipse probability is lower.

4. OBSERVATIONAL IMPLICATIONS

The close separation of stable stellar binaries implies a higher probability for detecting the eclipses. However,

the detection of eclipsing binaries depends sensitively on the data sampling and the eclipse duration. In this section, we consider these relevant observational parameters of the eclipses, which are useful in the search for stellar binaries. Similarly to the previous section, we adopt SO2 as an example.

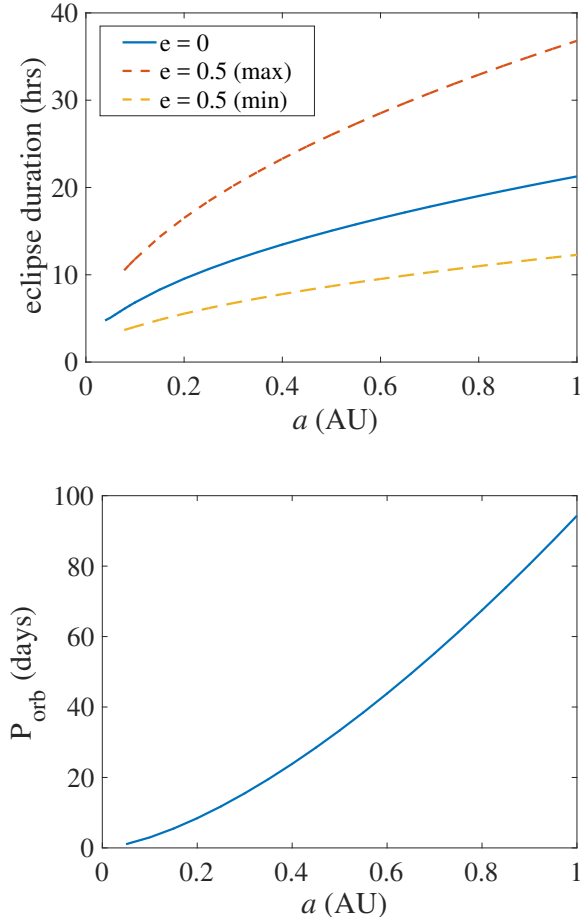


Figure 5. Upper panel: eclipse duration. Lower panel: orbital period of the stellar binary. The dashed lines in the upper panel correspond to the maximum and minimum eclipse duration for an eccentric orbit ($e = 0.5$). The eclipse durations of the binaries are mostly $\lesssim 1$ day (24 hrs) for $a \lesssim 0.5$ AU.

We first consider the duration of the eclipses, which can be written as: $P_{orb}/(\pi) \text{asin}[\sqrt{(R_1 + R_2)^2 - b^2}/a]$ for a circular orbit, where b is the sky projected impact parameter. We assume a zero impact parameter to estimate the duration. As shown earlier, the sum of the stellar radii depends weakly on the stellar binary mass ratio. Thus, we set $q = 1$ for the plots in Figure 5. The tidal disruption separation is 0.039 AU for the stellar binary. Thus, we only consider $a > 0.039$ AU for a circular stellar binary, and $a > 0.078$ AU for an eccentric stellar binary with $e = 0.5$.

The upper panel of Figure 5 shows the transit duration of the stellar binary as a function of semi-major axis. The transit duration is longer when a increases, and the duration is lower than one day for $a \lesssim 0.5$ AU. The lower panel of Figure 5 presents the stellar orbital period. The

eclipse duration to orbital period ratio varies from ~ 0.1 to 0.01 for a between 0.1 – 1 AU.

For an eccentric orbit, we calculated the transit duration numerically. The duration varies as the orbital phase changes, with larger values when the stars are near their apo-center. The dashed lines in the upper panel of Figure 5 illustrates the maximum and the minimum duration times for $e = 0.5$. This is obtained by uniformly sampling the binary orbit orientation and directly calculating the duration time according to the orbital phase when the stellar binaries eclipse. When the orbit is eccentric, the eclipse duration can exceed one day when $a \gtrsim 0.5$ AU. Roughly speaking, the ratio of the maximum duration time to the case when the orbit is circular is $\sim \sqrt{(1+e)/(1-e)}$, and the ratio for the minimum duration time is $\sim \sqrt{(1-e)/(1+e)}$, inversely proportional to the orbital velocity.

5. DISCUSSIONS

It is possible that some of the S-stars are tight stellar binaries. The close separation of the stable binary systems implies a higher eclipse probability along the line of sight. In this paper, we estimated the eclipse probability and the eclipse duration for the search of such possible binaries. Using SO2 as an example, we found the eclipse probability is $\sim 75\%$ if the stars are at their Roche lobe limit, and $\sim 30 - 50\%$ if the stellar binary semi-major axis is 0.1 AU, where the binary is stable against Kozai-Lidov oscillations. The eclipse probability is higher if the stellar binary is eccentric (reaching $\sim 50\%$ with $e = 0.5$) or when the orbit is highly misaligned relative to the orbit around Sgr A*. The eclipse duration ranges between $\sim 5 - 21$ hrs when a ranges between $\sim 0.1 - 1$ AU for circular orbits, and the duration can be longer for eccentric orbits.

Pfuhl et al. (2014) searched for spectroscopic and eclipsing binaries in the Galactic Center. Selecting average photometric error < 0.1 mag and periodic variabilities, only bright systems IRS 16SW and E60 are identified as binaries. In searching for spectroscopic binaries, only 13 brightest stars ($mk < 12$) with prominent emission/absorption lines were analyzed with precise radial velocity measurements, and IRS 16NW was identified as a binary. Future observations, such as with the James Webb Space Telescope (JWST) have the potential to observe near infrared sources with higher photometric precisions and help identify eclipsing binaries in the Galactic Center. The identification of stellar binaries in the S-cluster will provide valuable information on the dynamical processes leading to their formation.

ACKNOWLEDGMENTS

This work was supported in part by the Black Hole Initiative, which is funded by a grant from the John Templeton Foundation.

REFERENCES

- Alexander, T., & Hopman, C. 2009, ApJ, 697, 1861, 0808.3150
- Antonini, F., & Merritt, D. 2013, ApJ, 763, L10, 1211.4594
- Binney, J., & Tremaine, S. 1987, Galactic dynamics
- Eggleton, P. P. 1983, ApJ, 268, 368
- Gillessen, S., Eisenhauer, F., Fritz, T. K., Bartko, H., Dodds-Eden, K., Pfuhl, O., Ott, T., & Genzel, R. 2009, ApJ, 707, L114, 0910.3069

Ginsburg, I., Li, G., Naoz, S., & Loeb, A. in prep

Ginsburg, I., & Loeb, A. 2007, MNRAS, 376, 492, astro-ph/0609440

Hills, J. G. 1988, Nature, 331, 687

Kippenhahn, R., Weigert, A., & Weiss, A. 2012, Stellar Structure and Evolution

Kozai, Y. 1962, AJ, 67, 591

Lidov, M. L. 1962, Planet. Space Sci., 9, 719

Martins, F. et al. 2006, ApJ, 649, L103, astro-ph/0608215

Merritt, D., Gualandris, A., & Mikkola, S. 2009, ApJ, 693, L35, 0812.4517

Morris, M. 1993, ApJ, 408, 496

Naoz, S. 2016, ARA&A, 54, 441, 1601.07175

Naoz, S., & Ghez, A. in prep

Ott, T., Eckart, A., & Genzel, R. 1999, in Astronomical Society of the Pacific Conference Series, Vol. 186, The Central Parsecs of the Galaxy, ed. H. Falcke, A. Cotera, W. J. Duschl, F. Melia, & M. J. Rieke, 310

Pan, T., & Loeb, A. 2012, MNRAS, 425, L91, 1206.1050

Perets, H. B. 2009, ApJ, 698, 1330, 0802.1004

Perets, H. B., & Gualandris, A. 2010, ApJ, 719, 220, 1004.2703

Pfuhl, O., Alexander, T., Gillessen, S., Martins, F., Genzel, R., Eisenhauer, F., Fritz, T. K., & Ott, T. 2014, ApJ, 782, 101, 1307.7996

Prodan, S., Antonini, F., & Perets, H. B. 2015, ApJ, 799, 118, 1405.6029

Stephan, A. P., Naoz, S., Ghez, A. M., Witzel, G., Sitarski, B. N., Do, T., & Kocsis, B. 2016, MNRAS, 460, 3494, 1603.02709

Witzel, G. et al. 2014, ApJ, 796, L8, 1410.1884

—. 2017, ArXiv e-prints, 1707.02301

Yu, Q., & Tremaine, S. 2003, ApJ, 599, 1129, astro-ph/0309084